Geotech Geol Eng (2009) 27:699–711
DOI 10.1007/s10706-009-9269-9

ORIGINAL PAPER

Dynamic Analysis of Subway Structures Under Blast Loading

Huabei Liu

Received: 19 December 2008 / Accepted: 22 August 2009 / Published online: 17 September 2009

Abstract Public transit systems have become one of the targets of terrorist attacks using explosives, examples of which are the 1995 attack on Paris subway and the 2004 attack on Moscow subway. Considering the intense threats of terrorist attacks on subway systems in metropolitan areas, explicit three-dimensional Finite Element method was used to investigate the dynamic response and damage of subway structures under internal blast loading. The study was motivated by the fact that explosion in subway structure may not only cause direct life loss, but also damage the subway structure and lead to further loss of lives and properties. The study based on the New York subway system, and investigated the influences of various factors on the possible damage of subway tunnel, including weight of explosive, ground media, burial depth and characteristics of blast pressure. A mitigation measure using grouting to improve ground stiffness and strength was also analyzed. Considering the amount of explosive terrorists may use, the present study focused on small-diameter single-track tunnels, which are more vulnerable to internal blast loading and are common in New York City. Blast pressure from explosion was applied to lining surface assuming triangle pressure–time diagram, and the elasto-plasticity of ground and lining as well as their nonlinear interaction was taken into account in the numerical model. It is found from the numerical study that maximum lining stress occurred right after explosion, before the blast air pressure reduced to the atmospheric one, and it was more dependent on the maximum magnitude of air pressure than on the specific impulse, which is the area below the pressure–time curve. Small tunnels embedded in soft soil, with small burial depth, might be permanently damaged even by modest internal explosion that may be perpetuated by terrorists.

Keywords Subway structure · Explosion · Finite Element method · Dynamic analysis · Damage

H. Liu (✉)
Department of Civil Engineering, City College of New York/CUNY, 160 Convent Ave. ST 195, New York, NY 10031, USA
e-mail: hliu@ccny.cuny.edu

1 Introduction

Subway is used extensively in metropolitan areas around the world. It has also become one of the targets of terrorist attacks in recent years. Among the various schemes that terrorists may use, bombing is one prime option, examples of which include the 1995 attack on Paris subway and the 2004 attack on Moscow subway (Dix 2004). Very recently, the Department of Homeland Security of the United States issued a warning that terrorists may also target New York City Subway system using explosives.

Explosion inside a subway structure could directly threat the lives of people inside it; it might also damage the subway structure and cause further loss of lives and properties. Preventive measures should therefore be implemented not only to significantly reduce the possibility of terrorist attacks, but also to protect existing subway structures from collapse under internal blast loading; such internal blast loading should also be properly taken into consideration in the design of new subway structures. In the United States, the importance of this issue was addressed by the Blue Ribbon Panel on Bridge and Tunnel Security in their report (Blue Ribbon Panel on Bridge and Tunnel Security 2003), but the methods to evaluate the structure integrity of existing subways and the guidelines to design new underground structures taking into account the internal blast loading are still lacking.

This issue has seldom been investigated in the past. This is due to, first of all, the negligence of the problem in the days when the threat of terrorist attack was not as severe, and secondly, the very complicated characteristics of the problem, which includes dynamic ground-structure interactions, structure damage, nonlinear response of ground media, three-dimensional effects, and coupled fluid–structure interaction. Considering this complexity, small-scale experiments or analytical analyses generally cannot reveal the true mechanism. Instead carefully designed, sophisticated dynamic numerical method has the potential to accomplish the task.

Only limited related study can be found in the literature. Chille et al. (1998) investigated the dynamic response of underground electric plant subject to internal explosive loading using three-dimensional numerical method. Coupled fluid–solid interaction was considered in their study; however, the nonlinearity and failure of rock and concrete as well as the interaction between different solid media were not simulated. For traffic tunnels, Choi et al. (2006) used three-dimensional Finite Element method to study the blast pressure and resulted deformation in concrete lining. They found, through analysis of coupled fluid–solid interaction, that the blast pressure on tunnel lining was not the same as the CONWEP normally reflected pressure (Department of the Army, the Navy, and the Air Force 1990). The subjects of these two studies were both underground structures in rock mass, which are more resistant to internal blast loading than subway structures in soils. Lu et al. (2005) and Gui and Chien (2006), using Finite Element method, looked into the blast-resistance of tunnels in soft soil subject to external explosive loadings. There exist very few numerical studies investigating the dynamic and nonlinear response of subway structures subject to internal blast loading.

In this study, three-dimensional Finite Element program ABAQUS (Abaqus Inc 2004) was used to analyze the dynamic response and damage of subway structures in different ground media. The elasto-plasticity of ground media, possible damage of lining material and nonlinear interaction between lining and ground were taken into account in the numerical models. The numerical study was based on the subway system in New York City, considering its importance as well as its high risk of terrorist attack. At this stage, the coupled fluid–solid interaction of internal explosion in underground tunnels was not considered. Instead, the normally reflected pressure diagram assuming rigid solid surface, hereafter referred to as CONWEP reflected pressure, which was proposed by the Department of the Army, the Navy, and the Air Forces (1990), was used. The pressure was applied to the subway structure as impulse loading at appropriate location. The effects of incident angle on reflected pressure (Department of the Army, the Navy, and the Air Forces 1990; Smith and Hetherington 1994) were considered to obtain the impulse pressures at other locations. The possible effects of pressure reflection and superposition were also discussed.

Rocks (ranging from intact to highly fractured), dense sandy soil and saturated soft soil were considered in the numerical models as the ground media surrounding subway structures. These materials cover the possible ground media of New York Subway. According to the recommendations of Federal Emergency Management Agency (FEMA 2003), the equivalent explosive in a suit case ranges from 10 to 50 kg TNT, which is the possible explosive that terrorists might use in an attack targeting subway structure. With such amount of explosive, it is estimated that the damage on subway structure with large internal dimension would be small. Hence the present study focused on the dynamic response and damage of single-track subway tunnel, which is common to the subway system in New York City (Rossum 1985).

2 Finite Element Model

The Finite Element models were based on two parallel single-track subway tunnels in New York City (Ghaboussi et al. 1983). The inner diameter of the tunnels was simplified as 5 m, and their distance from center to center was 8 m. The tunnels were about 9 m below ground surface. However, other burial depths were also analyzed to investigate the influence. In order to fully consider the three-dimensional effects, large Finite Element model was used. Figure 1 shows the Finite Element mesh when the burial depth is 9 m. The model extended 50 m in the longitudinal direction of the tunnels, while the length and height of the model were 100 and 50 m, respectively. The Finite Element model was fixed at the base, and roller boundaries were imposed to the four sides.

2.1 Modeling of Materials

Considering the geological condition in New York City, subway tunnels in different ground media were analyzed. Intact rock mass (Manhattan Schist), average-quality rock mass, poor-quality rock mass, dense sandy soil, and saturated soft soil were considered. However, for all these cases, to simulate the fill right below ground surface, 3 m of soil was considered, the unit weight of which was 18.9 kN/m^3. Drucker–Prager elasto-plastic model (Abaqus Inc 2004) was used to model the rock media and saturated soft soil, but Cap model (Baladi and Sandler 1981; Mizuno and Chen 1981; Abaqus Inc 2004) was used to model the dense sand. Under modest blast loading that was considered in this study, it was estimated that the compression of rock materials was still elastic, hence the plastic volumetric-hardening was not simulated and Drucker–Prager elasto-plastic model without cap hardening was used to model the rock masses. However, plastic hardening of volume is critical to sandy soil under blast loading, and the dense sandy soil was simulated using Cap model. Regarding saturated soft soil, since undrained condition was assumed in the blast-resistance analysis, no volume change might occur during blast loading hence modeling its elasto-plastic shear deformation using Drucker–Prager model is adequate.

The model parameters for intact rock mass were based on those of real Manhattan Schist (Desai et al. 2005), and those for average-quality and poor-quality rock masses were based on the empirical parameters proposed by Hoek and Brown (1997). It is noted that Hoek and Brown (1997) also proposed the empirical parameters for intact rock mass, which is close to those for Manhattan Schist in Desai et al. (2005).

The undrained response of one saturated silt reported in Stark et al. (1994) was used to simulate

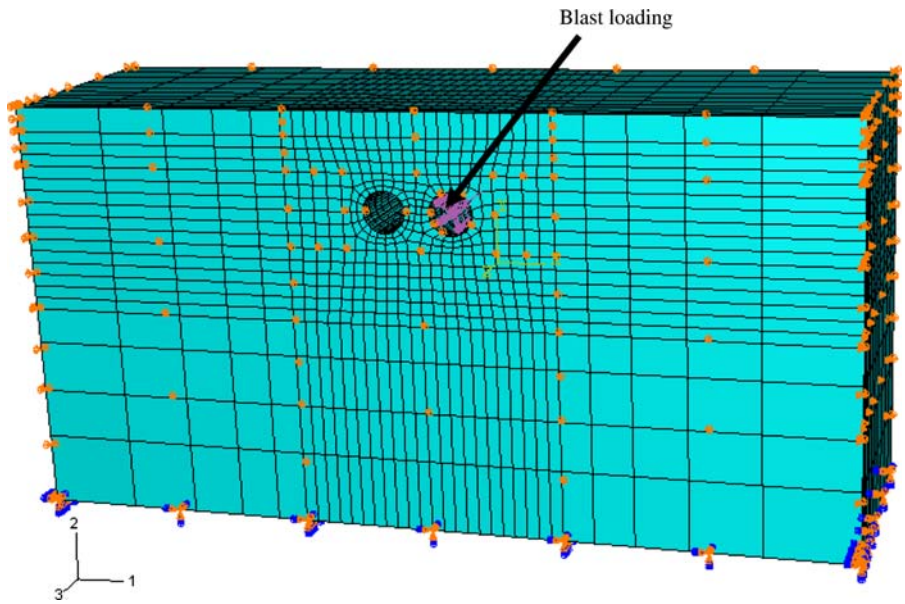

Fig. 1 Finite element mesh

the saturated soft soil that can be found in downtown Manhattan and some locations of Queens and Brooklyn in New York City. Undrained behavior is relevant for saturated soft soils subject to rapid blast loading since the movement of pore water is negligible under such circumstance. As can be seen in the subsequent section, the maximum response of tunnel occurred during blast loading. Hence although the dissipation of excess pore pressure after blast loading is sure to affect tunnel response, assuming undrained condition is considered to be adequate in the present study, since the objective is to investigate the maximum response and possible damage of subway tunnels. To model the behavior of dense sandy soil, the Cap model parameters of dense Ottawa sand that were calibrated in (Baladi and Sandler 1981; Mizuno and Chen 1981) were used as reference. It is noted that stress history and effective pressure can influence the stiffness and strength of soils, therefore, the Finite Element model was divided into layers, and each layer was assigned different model parameters based on the level of effective stress.

Under rapid blast loading, geomaterials like rock and soil exhibit rate-dependent behavior. For rock-like materials, experiments on concrete have shown that the increase of strength and stiffness under blast loading is not significant (Departments of the Army, the Navy, and the Air Forces 1990). With this in mind and also considering the fact that the rock parameters used in the present study were only representative, the stiffness and strength of rock masses were not adjusted for rate effects. The parameters in Desai et al. (2005) and Hoek and Brown (1997) were used directly in the dynamic analysis. On the other hand, the stiffness and strength of soils increase significantly under rapid loading (Jackson et al. 1980; Farr 1990; Ishihara 1996), although there have been conflicting conclusions regarding the amount of stiffness increase. Jackson et al. (1980) concluded that transient stiffness up to ten times the static one was found in their tests. However, Farr (1990) presented his test results, pointing out that very large stiffness increase at high strain rate was not possible, and that the very large values obtained in the former studies could be due to large measurement errors. In the present study, the transient stiffness and strength of both saturated soft soil and dense sandy soil were both assumed to be twice the static ones according to Farr (1990) and Ishihara (1996). However, parametric study was conducted to investigate the influence of soil stiffness and strength.

Another important aspect of geomaterial modeling is the dependence of strength on stress path. In this study, considering the ground stress condition under internal blast loading, the strengths of the geological materials were obtained considering plane-strain condition. The cohesion, friction angle and dilation angle were used to obtain d and tanβ for the constitutive models under the condition of plane strain, which is briefly discussed in Appendix A. Such assumption is only approximate, but it can considerably simplify the numerical analysis. The model parameters for the five ground media analyzed in this study are shown in Tables 1 and 2. Brief introductions of the Drucker–Prager elasto-plastic model and Cap model are given in Appendices A and B, respectively.

Table 1 Drucker–Prager model parameters for rocks and saturated soft soils

	Young's modulus E (MPa)	Poisson's ratio v	Cohesion c (MPa)	Friction angle ϕ (°)	Dilation angle ψ (°)	Unit weight γ (kN/m^3)
Manhattan Schist	33,600	0.128	6.6	50	12.5	24.0
Average—quality rock	9,000	0.25	3.5	33	4	24.0
Poor—quality rock	1,400	0.3	0.55	24	0	24.0
Saturated soft soil—Layer I[a]	5.6	0.495	38	0	0	20.0
Saturated soft soil—Layer II[a]	10	0.495	90	0	0	20.0
Saturated soft soil—Layer III[a]	16	0.495	150	0	0	20.0
Saturated soft soil—Layer IV[a]	23	0.495	170	0	0	20.0
Saturated soft soil—Layer V[a]	31	0.495	296	0	0	20.0

[a] Saturated soft soil Layers I–V are counted from top to bottom, the thicknesses of which are, $d_{\text{Layer I}} = 4.15$ m, $d_{\text{Layer II}} = 9$ m, $d_{\text{Layer III}} = 8.85$ m, $d_{\text{Layer IV}} = 10.5$ m, and $d_{\text{Layer V}} = 14.5$ m

Table 2 Cap model parameters for dense sandy soils

	Young's modulus E (MPa)	Poisson's ratio v	Cohesion c (MPa)	Friction angle ϕ (°)	W	D (1/MPa)	R	p_0^a (MPa)	Unit weight γ (kN/m^3)
Layer I[b]	146.72	0.3	0.0	43	0.0012	0.87	2.45	0.056	17.0
Layer II[b]	324.88	0.3	0.0	43	0.0012	0.87	2.45	0.124	17.0
Layer III[b]	759.80	0.3	0.0	43	0.0012	0.87	2.45	0.219	17.0
Layer IV[b]	792.78	0.3	0.0	43	0.0012	0.87	2.45	0.290	17.0
Layer V[b]	1,100.0	0.3	0.0	43	0.0012	0.87	2.45	0.418	17.0

[a] The initial location of hardening cap p_0 was assumed to be the average mean stress of the soil layer

[b] The division of soil layer is the same as that in Table 1

In New York City, cast iron was used extensively as tunnel lining in the early days (Rossum 1985). It was used in the present study as tunnel lining. The lining was simulated using shell elements, the stiffness and thickness of which were based on the real lining in Ghaboussi et al. (1983). Elasto-plastic model following von Mises failure criterion, i.e., $q - k = 0$, with k being the yield Mises stress and $q = \sqrt{\frac{1}{2}\left[(\sigma_1 - \sigma_2)^2 + (\sigma_1 - \sigma_3)^2 + (\sigma_2 - \sigma_3)^2\right]}$, was used to simulate the lining, the yield strength of which was based on that of grey cast iron (ASTM Standard A48 2008). According to Departments of the Army, the Navy, and the Air Forces (1990), the yield strength of steel increased slightly under blast loading but its stiffness is not affected. In the present study, the effects of rapid loading on the stiffness and strength of cast iron were not considered, considering both the possible small increase of strength and stiffness with loading rate and the degradation of cast-iron after many decades in service. The material properties of cast-iron lining are shown in Table 3.

The interaction between tunnel lining and the surrounding medium was modeled using thin-layer elements, which also followed Drucker–Prager elasto-plastic behavior. However, the strength of the thin-layer elements were reduced according to $\bar{c} = \frac{2}{3}c$, and $\tan\delta = \frac{2}{3}\tan\phi$, in which $\bar{c}$ and δ are the cohesion and friction angle of the interface between lining and surrounding geological medium, respectively, while c and ϕ are those of the geological medium. The stiffness of the interface elements was assumed to be the same as that of the ground medium and the dilation angle was assumed to be zero.

In the dynamic analysis, 5% viscous damping was considered for the geological materials while 2% was considered for the cast-iron lining.

Table 3 Material properties of the cast-iron lining

Young's modulus E (MPa)	Poisson's ratio v	Yield Mises stress k (MPa)	Unit weight γ (kN/m^3)	Equivalent thickness (cm)
140,000	0.2	173.0	78.0	13

2.2 Modeling of Blast Loading

Coupled fluid–solid interaction of an explosion inside a tunnel was not modeled in the present study. Instead, the reflected pressure on a rigid plane surface that was proposed by the Departments of the Army, the Navy, and the Air Forces (1990), i.e., the CONWEP reflected pressure, was used and applied to the tunnel lining as impulse loading. The explosive was assumed to be spherical and explode at the center of one tunnel. The internal surface of the tunnel was divided into five regions. The first region, which was closest to the explosive and next to the front boundary of the Finite Element model, was 1 m long in the longitudinal direction. In this region, the impulse pressure was assumed to be the normally reflected pressure p_r (Departments of the Army, the Navy, and the Air Forces 1990; Smith and Hetherington 1994). The pressures acting on the second region (1 m long), the third region (6 m long), and the fourth region (8 m long) were obtained by considering the incident angle at the center of each region as well as the distance to the assumed explosive. According to Smith and Hetherington (1994), beyond the fourth region, which was more than 14 m away from the explosive and the incident angle is larger than 80° in a tunnel whose diameter is 5 m, the blast pressure was already very

small. Therefore, the tunnel surface in the fifth region was assumed to be free of loading.

The pressure–time curve was assumed to be of triangular shape, the duration of which was obtained from the CONWEP reflected pressure diagram. Four explosive amounts, 10, 30, 50 and 75 kg TNT, were analyzed in this study, the durations of which for the normally reflected case were 1.8, 1.6, 1.3 and 0.8 ms, respectively. The maximum normally reflected pressures, which were applied in the first region, were 4.0, 6.0, 10 and 15 MPa, respectively, for the four explosives considered. The maximum pressures were 3.2, 4.5, 7.5 and 13 MPa on the second region, 0.6, 1.0, 1.5 and 1.7 MPa on the third region, and 0.07, 0.1, 0.15 and 0.25 MPa on the fourth region were, respectively, according to Smith and Hetherington (1994).

According to Choi et al. (2006), the reflection and superposition of air pressure in a tunnel due to internal explosion is different from the reflected one on rigid surface. The maximum pressure magnitude is smaller but the duration is much longer. The specific impulse, i, which is the area beneath the pressure–time curve, is larger than the reflected one i_r. In order to investigate the influences, assumed specific impulse and maximum pressure magnitude were also analyzed in this study, based on the explosion of a 30 kg TNT equivalent explosive.

2.3 Procedure of Analysis

Dynamic explicit analysis was used to capture the transient and nonlinear behavior of the tunnel—ground system. The analysis was carried out in two steps. The first step obtained the initial stress state before explosion, and the second step analyzed the dynamic response under blast loading. In order to obtain the initial static stress state, dynamic explicit analysis was conducted with linearly increasing gravity load over a long period of time in order to simulate a quasi-static condition. Static standard analysis was carried out to check whether the initial stress state obtained from explicit dynamic analysis was similar to those from static analysis. A difference of less than 10% was found. Blast analysis was then conducted for 50 ms, with very small time-step of 1.0×10^{-3} ms. Test runs were carried out to determine the length of analysis and time step and it was found that the above two parameters were adequate in capturing the major response.

Altogether about 60 analyses were conducted to closely study the dynamic response and damage of subway tunnels subject to internal blast loading. The effects of explosive weight, ground media, burial depth, blast loading characteristics, and possible mitigation measure, were investigated. Table 4 summaries the analyzing cases. The analysis focused on the maximum Mises stress ($q = \sqrt{\frac{1}{2}\left[(\sigma_1-\sigma_2)^2+(\sigma_1-\sigma_3)^2+(\sigma_2-\sigma_3)^2\right]}$) in the tunnel lining, which determines the yield and damage of the lining material.

It is understood the thickness of tunnel lining may be different with different burial depths or different ground media. However, in order to look into the influences of various parameters, it was assumed to be the same for different cases in this study. It should be noted that the analyzed tunnel lining was based on an actual one, which was 9 m below ground surface in sandy soil (Ghaboussi et al. 1983). With this lining, the maximum Mises stresses under gravity loading in all the cases were all much smaller than the yield stress, and their differences were smaller than 10 MPa.

3 Results of Numerical Simulation

3.1 General Response

Under the internal blast loading, the tunnel—ground system exhibited similar response mode, although the magnitudes were significantly different with different tunnel, ground, or explosive parameters. The responses of the system when the tunnels were 9 m below ground surface in saturated soft soil and subject to a blast-loading of 50 kg-TNT explosion (Base case in Table 4) are discussed in this subsection.

Under the blast loading, the Mises stress of the tunnel with internal explosion increased dramatically, which was accompanied with extreme lining-vibration. Figure 2a shows the change of maximum Mises stress in the lining with time. It increased dramatically immediately after explosion, reached the peak at about 1 ms, and was followed by a fluctuation with overall decreasing magnitude. The Mises-stress distribution in the tunnel lining at about 1 ms is shown in Fig. 2b. The large stress concentrated at the section close to the explosion. And by observing the plastic

Table 4 Cases of numerical analysis

	Explosive weight (kg-TNT)	Ground media	Burial depth (m)	Specific impulse and peak blast pressure
Base case	50	Soft soil	9	CONWEP
Different weights of explosives	10, 30, 50, 75	Strong rock, medium rock, weak rock, dense sand, soft soil	9	CONWEP
Effect of ground stiffness and strength	30, 50	Soft soils with different strength/stiffness	9	CONWEP
Effect of burial depth	30, 50	Soft soil	3, 5, 9, 15,19	CONWEP
Mitigation measure	50	Soft soils with various thickness of grouting around tunnels	9	CONWEP
Influence of peak blast pressure and specific impulse	50	Soft soil	9	Specific impulse: 1.5, 2.0, 2.5 times of CONWEP; peak pressure: 0.5, 0.6, 0.667, 0.75 of CONWEP

strain in the lining, it is found that in this case the lining was already damaged due to blast loading, although only at limited location,

Figure 3 shows the Mises-stress wave in the soil surrounding the tunnels. 0.5 ms after explosion, the shear stress concentrated mainly in the thin-layer of soil in contact with the tunnel; at 0.9 ms, the shear stress wave started to travel to the surrounding soil; but at 1.9 ms, shear stress in the thin-layer of soil increased again due to lining vibration; and at 2.3 ms, the new shear stress wave traveled to the surrounding soil. Such phenomenon continued until the end of analysis but with decreasing stress magnitude. It should be pointed out that the blast loading on the tunnel surface stopped at 1.3 ms in this case.

In this study, absorbing boundary was not used to eliminate stress-wave reflection from boundary, which is adequate for the problem investigated. As can be seen in Fig. 2a, the maximum response in the lining occurred during blast loading. With the large Finite Element model used in the numerical simulation, wave reflection did not affect the main response during blast loading and the short period afterwards, as shown in Fig. 2a.

The stress of the tunnel lining that is parallel to the one with explosion was generally small in all the cases and did not cause damage. And as the possible damage of tunnel lining is the main objective of this study, only the maximum lining shear stress (Mises stress) in the tunnel with explosion will be discussed hereafter.

3.2 Lining Stresses with Different Weights of Explosive

As can be expected, with an increase in the weight of explosive, the maximum shear stress in the lining increased, as shown in Fig. 4. However, the rate of increase was rather different for different ground media. The increase was much more significant for subway tunnels in soils. In saturated soft soil, some locations started to yield when the explosive was more than 50 kg TNT. In dense sandy soil, the lining stress was smaller but the increase with explosive-weight was also significant, and when the explosive was 75 kg TNT, the lining stress approached the yield one. The lining stress was much smaller if the tunnel was embedded in rock, so was the increase. The lining was still far from being damaged if the ground was rock, even with 75 kg-TNT explosive.

Since it is not likely for terrorists to use very large amount of explosive in an attack targeting subway tunnels, the evaluation of lining damage due to possible terrorist attack using explosive can focus on those in soft soils.

3.3 Effect of Ground Stiffness and Strength

As already indicated in Fig. 4, the lining stress was directly related to ground media. In order to identify the most important influencing factor, parametric study was conducted to investigate the influences of ground strength and ground stiffness, respectively. The tunnels

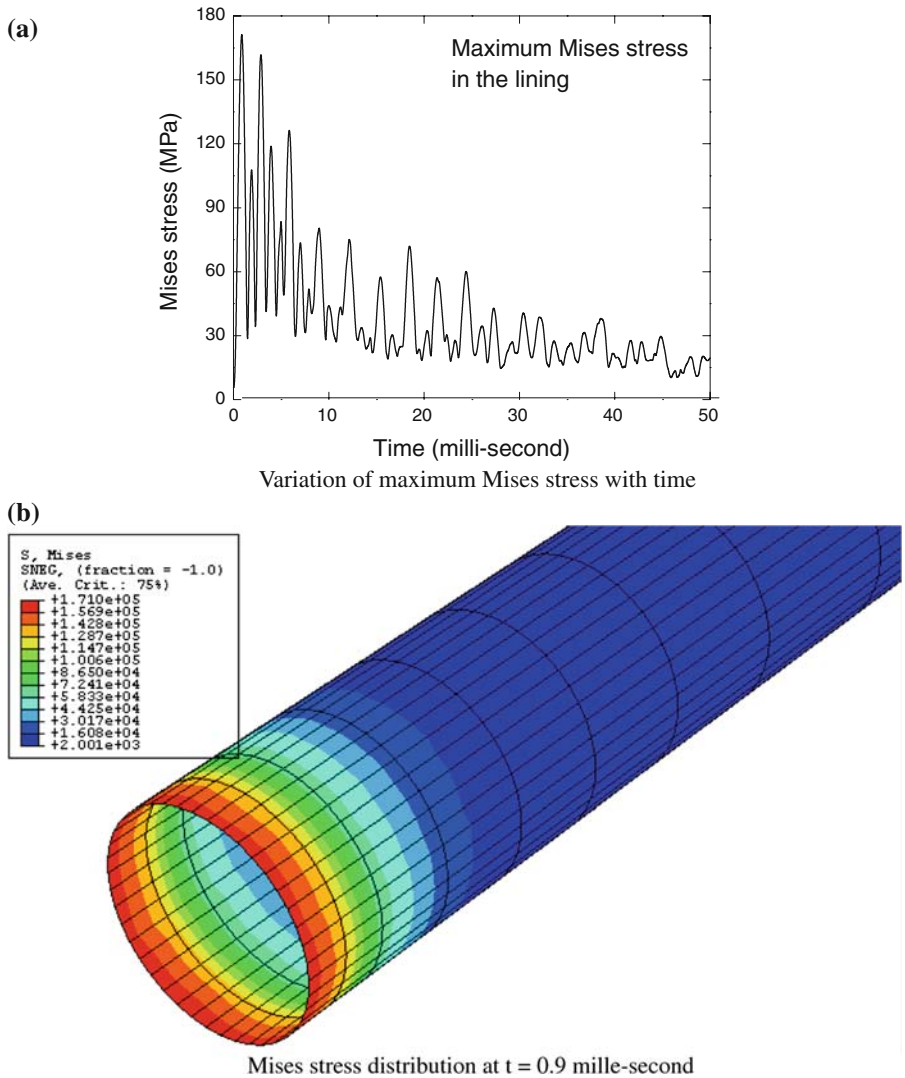

Fig. 2 Mises stress in the tunnel lining. **a** Variation of maximum Mises stress with time. **b** Mises stress distribution at $t = 0.9$ ms

in soft soils were analyzed, with explosives of both 30 and 50 kg TNT. A series of analysis was firstly carried out by varying soil stiffness but keeping soil strength constant, followed by another series with constant soil stiffness but varying soil strength. The soil stiffness or strength in each layer was increased or decreased proportionally to investigate their influences.

As shown in Fig. 5a, with a decrease in the soil stiffness, the maximum lining stress increased significantly, under either 30 kg-TNT explosion or 50 kg-TNT explosion. The lining might be permanently damaged if the soil stiffness was adequately small. On the other hand, under modest blast loading, the lining stress was only very slightly influenced by the soil strength in the range investigated, as shown in Fig. 5b. Thus it can be seen that even in soft soil, ground stiffness is more important that ground strength for a subway tunnel subject to terrorist attack using explosive.

3.4 Effect of Burial Depth

The subway tunnels in saturated soft soil, subject to blast loading of either 30 or 50 kg-TNT explosive were still used to investigate this effect. Increasing the burial depth of subway tunnel enhances the

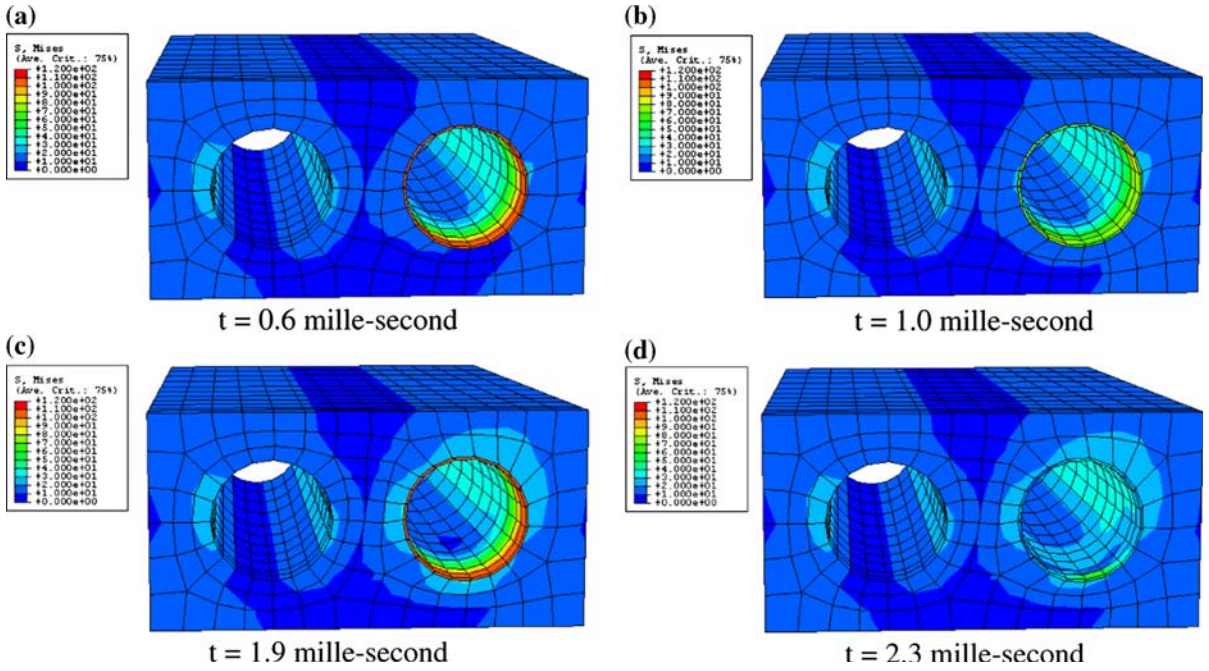

Fig. 3 Mises stress distribution in the soil around the tunnels

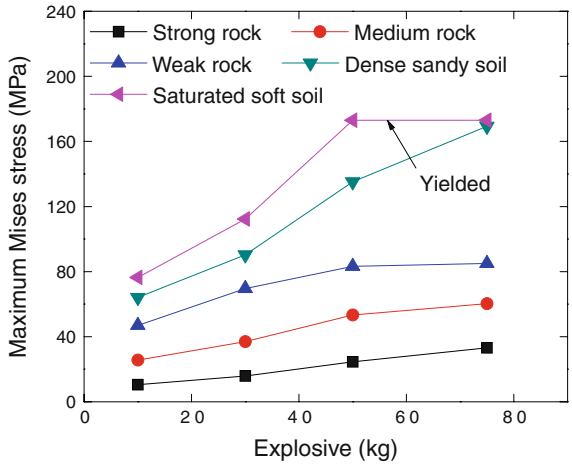

Fig. 4 Effects of explosive weight on lining stress

confinement on the tunnel, hence reduces the maximum lining stress under internal blast loading, as can be seen in Fig. 6. The change in lining stress was not linear, however, the lining stress and damage was more sensitive to burial depth when it was small. These results indicate that it is more necessary to evaluate the blast-resistance of subway tunnel with small burial depth.

3.5 Possible Mitigation Measure

As can be seen from Sects. 3.2–3.4, under the same internal blast loading, lining stress and damage were dependent on the effective confinement imposed by the ground. For subway tunnels in soft soil, if the burial depth is not adequately large, there is large probability that lining may be severely damaged under modest internal blast loading, which could be perpetuated by a terrorist attack using explosive.

With this in mind, a mitigation measure can be identified to increase the blast-resistance of subway structures. The soft soil close to the tunnels could be grouted to improve its stiffness and strength. Figure 7 shows the lining stresses under 50 kg-TNT explosion, with different thicknesses of improved soil. The stiffness and strength of the improved soil were assumed to be the same as those of the poor-quality rock in Table 1. It can be seen that, with just 1 m of soil around the tunnels improved to the target stiffness and strength, the maximum lining stress decreased significantly.

Grouting to improve the stiffness and strength of soft soil around subway tunnel can therefore be considered as a probable measure to increase significantly the blast-resistance of subway structure. Although this

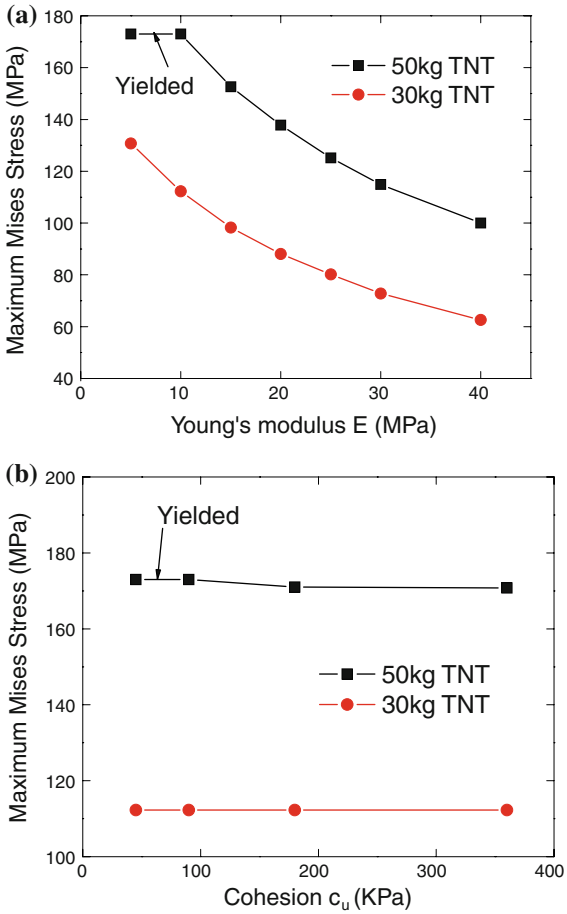

Fig. 5 Influences of soil stiffness and strength on lining stress (Shown on the *horizontal axes* are those of soil Layer II that is around the tunnels). **a** Effects of soil stiffness. **b** Effects of soil strength

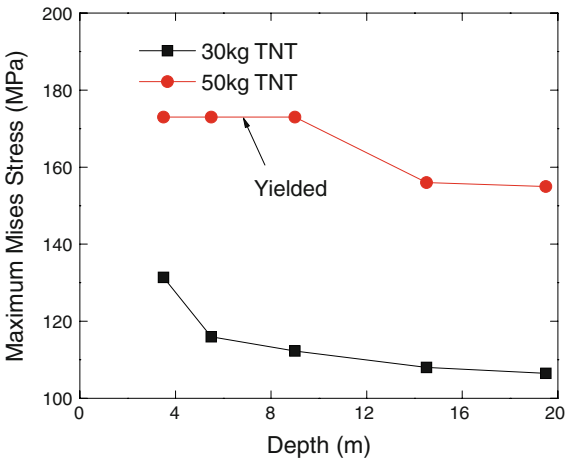

Fig. 6 Effects of burial depth on lining stress

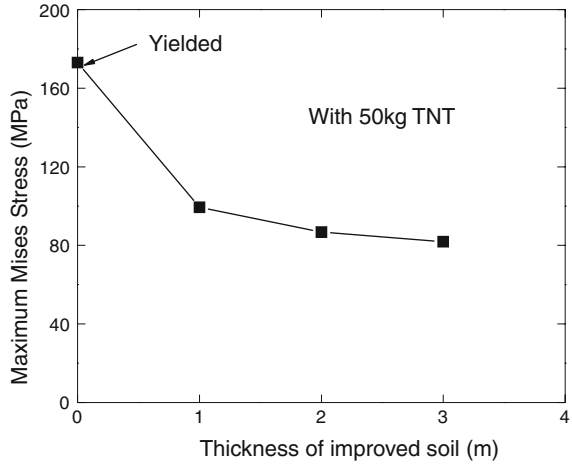

Fig. 7 Effectiveness of soil improvement on reduction of lining stress

measure could be costly to carry out, it could also bring other benefits such as higher earthquake—resistance, hence it might still be an acceptable option under certain circumstances.

3.6 Influence of Peak Blast Pressure and Specific Impulse

Reflection and superposition of air pressure due to explosion inside a tunnel generally lead to prolonged blast pressure on lining surface but the maximum pressure-magnitude is generally smaller than the normally reflected one on rigid surface. The specific impulse i, which is the area below the blast-pressure vs. time curve, and the maximum pressure–magnitude p, depend on the intense of explosion, tunnel diameter, ground condition, lining stiffness and other minor factors. In order to check the validity of the assumption in this study, blast pressures other than the assumed one were analyzed. Based on the reflected pressure on rigid surface by an explosion of 30 kg-TNT, the specific impulse i was increased to 1.5, 2.0 and 2.5 times of i_r, which is the CONWEP reflected specific impulse, but the maximum blast pressure was reduced to 0.75, 0.667, 0.6 and 0.5 of p_r, which is the CONWEP reflected pressure. The blast pressures were still applied to the appropriate locations on lining surface and the resulted maximum lining stress was compared. Figure 8a illustrates the four blast pressures and the original one when $i = 2.5 * i_r$.

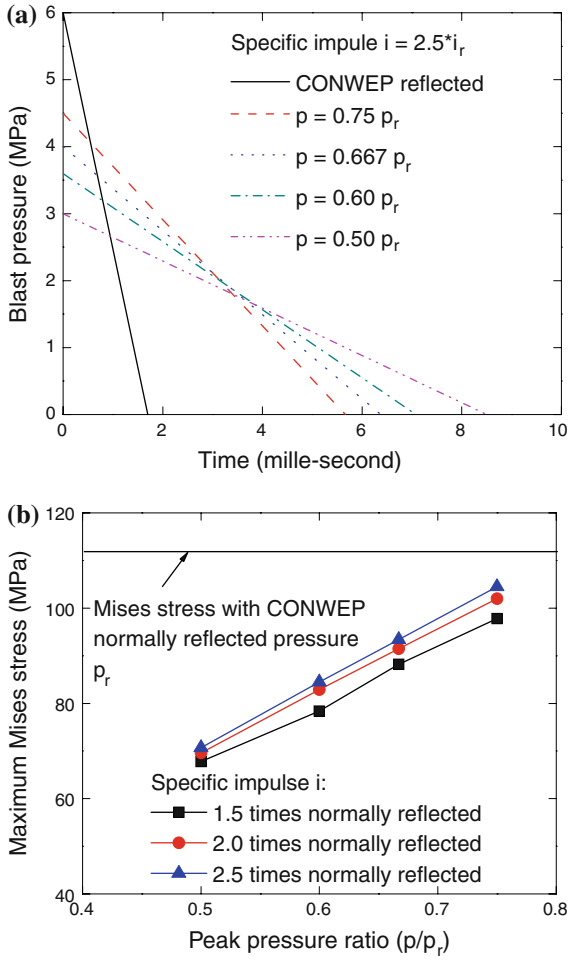

Fig. 8 Effects of blast-pressure characteristics on lining stress. **a** Blast pressure diagrams. **b** Lining stress

Figure 8b shows the change of lining stress with specific impulse and maximum pressure. The maximum lining stress under the CONWEP reflected pressure is also shown in the figure. It can be seen that among the two parameters of the blast pressure, the maximum magnitude was more important. And even when $i = 2.5 * i_r$ but $p = 0.75 * p_r$, the induced maximum lining stress was still smaller than that by CONWEP reflected pressure. It is also worth pointing out that the maximum lining stress occurred at about 1 ms for all the cases.

These results show that using CONWEP reflected pressure to analyze the blast-resistance of subway structures under internal blast loading could be conservative. However, definite conclusion can only be obtained with coupled fluid–solid interaction analysis.

4 Conclusions and Discussions

Using explicit dynamic Finite Element method, the nonlinear response of subway tunnels under internal blast loading was analyzed. The analysis was carried out under the present context of threats of terrorist attack on public transit systems using explosives. Such attack, if perpetuated, could not only lead to direct life loss, but also damage the subway structure, such as those in New York City, and caused indirect loss of lives and properties. Considering the possible amount of explosive terrorists may use, the present study focused on single-track subway tunnels that are of smaller diameter and more vulnerable to internal explosion. The study also focused on subway tunnels lined with cast iron since they are common in New York City.

Coupled fluid–solid interaction was not considered at this stage. Instead approximate approach using reflected blast pressure on rigid surface was used. The pressure was applied to the lining surface at appropriate locations as blast loading. The effects of explosive weight, ground medium, and burial depth of tunnels were investigated, based on which a possible mitigation measure was proposed. The approximation of assumed blast pressure was also analyzed. Based on the extensive numerical simulation, the following conclusions can be obtained:

1. Under internal blast loading, the maximum lining stress that may cause damage occurred at the section closest to the explosion and it occurred immediately after explosion, before the blast pressure on lining surface reduced to zero. The lining stress then fluctuated continuously, but with decreasing magnitude, due to lining vibration.
2. Ground stiffness had significant influence on lining stress and damage. Lining stress increased significantly if the tunnels were embedded in soft soils. On the other hand, under modest blast loading that might be perpetrated by terrorists on subway system, the strength of ground, in the normal range, had only slight influence on lining stress.
3. Burial depth affected significantly the maximum lining stress under internal blast loading. With small burial depth, due to the low confinement from ground, lining stress could be significantly large and the tunnel could be severely damaged even with modest internal explosion.

4. Grouting to improve the stiffness of soil around subway tunnel could be an effective mitigation measure to increase blast resistance.

Based on these conclusions, it can be seen that while evaluating blast-resistance of subway structures, attentions should be given to those with small diameter, embedded in soft soil and with small overburden soil layer. Appropriate mitigation measure may be necessary for critical tunnel sections with these characteristics, even if the probability of such attacks is small. Similar principle also applies to the design of new subway structures, which is advised to take into account blast loading in the United States by the Blue Ribbon Panel on Bridge and Tunnel Security (2003) appointed by American Association of State Highway and Transportation Officials (AASHTO) and Federal Highway Administration (FHWA).

The present study also found that the use of reflected pressure on rigid surface might be conservative in calculating lining stress and evaluating tunnel damage. Coupled fluid–solid analysis is necessary to obtain a definite conclusion that could be used in practice, which will be carried out in the next stage of study.

Acknowledgments The present study was supported by the United States Department of Transportation (USDOT) through a mini-grant awarded to the author by University Transportation Research Center—Region II. The support is gratefully acknowledged.

Appendix A

The yield criterion for Drucker–Prager model is based on the shape of the yield surface in the meridian plane, which is defined as:

$$f = q - p\tan\beta - d = 0 \tag{1}$$

in which q is the Mises stress, $p = \frac{1}{3}(\sigma_1 + \sigma_2 + \sigma_3)$ is the mean stress, and β and d are model parameters that are related to the cohesion c and friction angle ϕ of soil. Non-associated flow rule can be used, with the plastic-potential function expressed as:

$$g = q - p\tan\psi \tag{2}$$

Linear elastic behavior can be used together with the Drucker–Prager plasticity, which is defined by the Young's modulus E and Poisson's ratio v.

Under plane strain condition, the parameters β and d can be obtained from cohesion c and friction angle ϕ of soil using the condition of $\varepsilon_2 = 0$ (Abaqus Inc 2004)

$$\sin\phi = \frac{\tan\beta\sqrt{3(9-\tan^2\psi)}}{9-\tan\beta\tan\psi} \tag{3}$$

$$c\cos\phi = \frac{\sqrt{3(9-\tan^2\psi)}}{9-\tan\beta\tan\psi}d \tag{4}$$

Appendix B

The yield surface for the Cap model in the meridian plane used in this study is the same as that of Drucker–Prager model, as shown in Eq. 1. The cap yield surface is defined as:

$$f_c = \sqrt{(p-p_a)^2 + \left[\frac{Rq}{(1+\alpha-\alpha/\cos\beta)}\right]^2} - R(d+p_a\tan\beta) = 0 \tag{5}$$

In Eq. 5, R, d and β are model parameters, among which β and d are obtained from cohesion c and friction angle ϕ of soil using Eqs. 3 and 4 if plane-strain condition is assumed. α is a small constant, which is given as 0.01 in the present study. p_b is the parameter that governs the hardening of cap and is expressed as:

$$p_a = \frac{p_b - Rd}{1 + R\tan\beta} \tag{6}$$

in which p_a is related to the plastic volumetric strain under isotropic compression:

$$\varepsilon_v^p = W\{1 - \exp[-D(p_a - p_0)]\} \tag{7}$$

W and D are both material constants.

References

Abaqus Inc (2004) ABAQUS/standard user's manuals, version 6.4. Abaqus Inc, Providence

ASTM Standard A48 (2008) Standard specification for gray iron castings. ASTM International, West Conshohocken. doi: 10.1520/A0048_A0048M-03R08

Baladi GY, Sandler IS (1981) Examples of the use of the cap model for simulating the stress–strain behavior of soils. In: Proceedings of the workshop on limit equilibrium, plasticity and generalized stress–strain in geotechnical engineering, pp 649–710

Blue Ribbon Panel on Bridge and Tunnel Security (2003) Recommendations for bridge and tunnel security. Available online at http://www.fhwa.dot.gov/bridge/security/brptoc.cfm

Chille F, Sala A, Casadei F (1998) Containment of blast phenomena in underground electrical power plants. Adv Eng Softw 29:7–12

Choi S, Wang J, Munfakh G, Dwyre E (2006) 3D Nonlinear blast model analysis for underground structures. In: Proceedings of geocongress 2006, Paper No. 206

Departments of the Army, the Navy, and the Air Forces (1990) Structures to resist the effects of accidental explosions. US Army Technical Manual TM 5-1300

Desai D, Naik M, Rossler K, Stone C (2005) New York subway caverns and crossovers—a tale of trials and tribulations. In: Proceedings rapid excavation and tunneling conference (RETC) 2005, pp 1303–1314

Dix A (2004) Terrorism—the new challenge for old tools. Tunn and Tunn Int 36(10):41–43

Farr JV (1990) One-dimensional loading-rate effects. J Geotech Eng ASCE 12:119–135

Federal Emergency Management Agency (FEMA) (2003) Reference manual to mitigate potential terrorist attacks against buildings. FEMA 426

Ghaboussi J, Hansmire WH, Parker HW, Kim KJ (1983) Finite element simulation of tunneling over subways. J Geotech Eng ASCE 109:318–334

Gui MW, Chien MC (2006) Blast-resistant analysis for a tunnel passing beneath Taipei Shongsan airport—a parametric study. Geotech Geol Eng 24:227–248

Hoek E, Brown ET (1997) Practical estimates of rock mass strength. Int J Rock Mech Min Sci 34:1165–1186

Ishihara K (1996) Soil behavior in earthquake geotechnics. Clarendon Press, Oxford

Jackson JG, Ehrgott JQ, Rohani B (1980) Loading rate effects on compressibility of sand. J Geotech Eng Div ASCE 106:839–852

Lu Y, Wang Z, Chong K (2005) A comparative study of buried structure in soil subjected to blast load using 2D and 3D numerical simulations. Soil Dyn Earthq Eng 25:275–288

Mizuno E, Chen WF (1981) Plasticity models for soils—theory and calibration. In: Proceedings of the workshop on limit equilibrium, plasticity and generalized stress–strain in geotechnical engineering, pp 553–589

Rossum L (1985) New York City transportation tunnels—case histories and designer's approach. Munic Eng J 71:1–24

Smith PD, Hetherington JG (1994) Blast and ballistic loading of structures. Butterworth-Heinemann, Oxford

Stark TD, Ebeling RM, Vettel JJ (1994) Hyperbolic stress–strain parameters for silts. J Geotech Eng ASCE 120: 420–441